Chemosphere 345 (2023) 140399

Contents lists available at ScienceDirect

Chemosphere

journal homepage: www.elsevier.com/locate/chemosphere

Physiology-informed toxicokinetic model for the zebrafish embryo test developed for bisphenols

Ioana Chelcea [a], Carolina Vogs [b,c], Timo Hamers [d], Jacco Koekkoek [d], Jessica Legradi [d], Maria Sapounidou [a], Stefan Örn [b], Patrik L. Andersson [a,*]

[a] Department of Chemistry, Umeå University, SE-901 87, Umeå, Sweden
[b] Department of Biomedical Sciences and Veterinary Public Health, Swedish University of Agricultural Sciences, Box 7028, SE-75007, Uppsala, Sweden
[c] Institute of Environmental Medicine, Karolinska Institutet, SE-171 65, Solna, Sweden
[d] Amsterdam Institute for Life and Environment (A-LIFE), Vrije Universiteit Amsterdam, 1081, HV Amsterdam, the Netherlands

HIGHLIGHTS

- BPA, BPZ and BPAF time-dependent concentrations were measured in ZFE.
- Developed ZFE kinetic model included processes of epiboly, metabolism and perfusion.
- Bayesian inference modelling was applied for parameterization.
- Model predicted majority of data for BPA, BPAF, BPF and TBBPA within a 2-fold error.
- Estrogenicity higher for BPAF, BPC, BPB and BPZ than BPA considering dose at target.

GRAPHICAL ABSTRACT

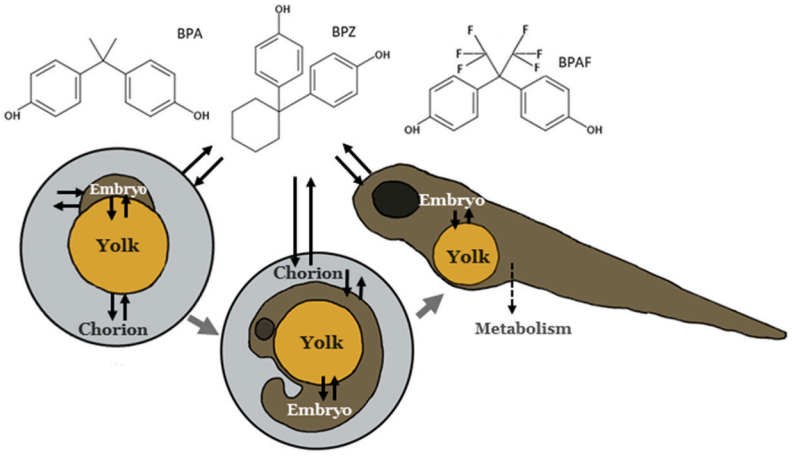

ARTICLE INFO

Handling editor: Marisa Passos

Keywords:
Embryo
PBTK
Zebrafish
Bisphenols
Endocrine disruptors

ABSTRACT

Zebrafish embryos (ZFE) is a widely used model organism, employed in various research fields including toxicology to assess e.g., developmental toxicity and endocrine disruption. Variation in effects between chemicals are difficult to compare using nominal dose as toxicokinetic properties may vary. Toxicokinetic (TK) modeling is a means to estimate internal exposure concentration or dose at target and to enable extrapolation between experimental conditions and species, thereby improving hazard assessment of potential pollutants. In this study we advance currently existing TK models for ZFE with physiological ZFE parameters and novel experimental bisphenol data, a class of chemicals with suspected endocrine activity. We developed a five-compartment model consisting of water, plastic, chorion, yolk sack and embryo in which surface area and volume changes as well as the processes of biotransformation and blood circulation influence mass fluxes. For model training and validation, we measured internal concentrations in ZFE exposed individually to BPA, bisphenol AF (BPAF) and Z (BPZ).

* Corresponding author.
E-mail address: patrik.andersson@umu.se (P.L. Andersson).

https://doi.org/10.1016/j.chemosphere.2023.140399
Received 4 May 2023; Received in revised form 26 July 2023; Accepted 8 October 2023
Available online 13 October 2023

Bayesian inference was applied for parameter calibration based on the training data set of BPZ. The calibrated TK model predicted internal ZFE concentrations of the majority of external test data within a 5-fold error and half of the data within a 2-fold error for bisphenols A, AF, F, and tetrabromo bisphenol A (TBBPA). We used the developed model to rank the hazard of seven bisphenols based on predicted internal concentrations and measured *in vitro* estrogenicity. This ranking indicated a higher hazard for BPAF, BPZ, bisphenol B and C (BPB, BPC) than for BPA.

1. Introduction

Endocrine disrupting environmental pollutants are of emerging concern, given their potential effects on both humans and wildlife (WHO/UNEP, 2012). In order to assess their hazards, either *in vitro* or *in vivo* methods have been employed. *In vitro* methods allow detailed studies on molecular initiating events (MIEs) of the adverse outcome pathway (AOP) to assess endocrine disrupting effects.(Marty et al., 2011) Using *in vivo* methods is a more accurate approach to assess chemical hazard as they take into account toxicokinetic processes of chemicals leading to dose at target as well as crosstalk in cellular signaling. However, animal testing is often ethically questionable, time-consuming, expensive, unsuitable for high throughput screening and provide limited information on mechanism of action.

The zebrafish embryo (ZFE) is gaining traction as a model organism for toxicity testing in endocrine research. The ZFE is a well-characterized model organism, and shares many gene and protein homologies with humans which enables species extrapolation (Scholz et al., 2008). In addition, the ZFE is considered an alternative non-animal test until free-feeding that allows high throughput testing since they are easy to maintain. Zebrafish have a high rate of reproduction making ZFE readily available, and environmental pollutants and pharmaceuticals have been documented to intervene with developmental trajectory, by inducing endocrine-mediated neurodevelopmental effects (Muncke and Eggen, 2006; Segner, 2009; Wang et al., 2011; d'Amora and Giordani, 2018; Mu et al., 2018; Gao et al., 2022).

Observed adverse outcomes in embryos related to disruption of endocrine systems are dependent on both the intrinsic properties of chemical to cause the toxic effect but also their ability to reach the target of toxicity (Punt et al., 2020). It has been discussed that differences in observed ZFE toxicity between perfluorinated compounds may stem from uptake differences rather than intrinsic toxicity (Vogs et al., 2019). Thus, understanding the toxicokinetic processes and internal dose are important requirements to extrapolate toxicity between *in vitro* systems as well as different organisms in order to interpret differences in sensitivity (Escher and Hermens, 2002). Yet, measuring internal concentrations in ZFE is not commonly done as it involves labor- and resource-intensive methods including advanced analytical chemistry (Gibert et al., 2011; Moreman et al., 2017). An alternative approach is to develop and apply toxicokinetic (TK) models as a non-animal methodology that enables prediction of the dose reaching embryos. A few TK models for ZFE have been published in recent years that range from simple one-compartment models to those including several organs (Kühnert et al., 2013; Brox et al., 2016; Bittner et al., 2019; Vogs et al., 2019; Halbach et al., 2020; Siméon et al., 2020; Billat et al., 2022; Warner et al., 2022). Limitations of these models include both physiology and chemical applicability as model calibration is chemical-specific. Additionally, minimal measured physiological data is available for embryos.

In the present study we aimed to develop a toxicokinetic model for ZFE using available measured physiological data from literature. In particular we wanted to advance currently existing models to include physiology and processes that have previously not been accounted for, such as epiboly, blood circulation and metabolism. The model was calibrated for bisphenols as a class of organic pollutants with widely documented endocrine properties. Novel experimental data was generated including time-course internal concentrations in ZFE of bisphenol A, AF and Z (BPA, BPAF, BPZ). In addition, a Bayesian inference protocol was used to calibrate unknown parameters and a sensitivity analysis was conducted to identify the most critical parameters. Finally, the developed toxicokinetic model was validated using an external test set, and applied in a hazard analysis of bisphenols where measured estrogen receptor (ER) activity was related to predicted internal concentrations.

2. Materials and methods

2.1. ZFE exposure regime

BPA (CAS 80-05-7), BPAF (CAS 1478-61-1) and BPZ (CAS 843-55-0) in crystal form were first dissolved in pure DMSO and then in ZFE water aiming for a final working solution with nominal concentration of 17 μM for BPA, 3 μM for BPAF and 3 μM BPZ. These concentrations were selected as 25% of the ZFE LC_{50} as reported previously (Tišler et al., 2016; Liu et al., 2021). The final measured water concentrations were 21 μM for BPA, 2.9 μM for BPAF and 5.8 μM for BPZ in 0.01% DMSO.

Exposure was performed starting at 4 h post fertilization (hpf) until 120 hpf. Biological control groups included ZFE exposed to 0.01% DMSO and ZFE exposed to ZFE water as well as a chemical control with just compound and no embryo in order to test chemical stability and losses. All well plates were incubated at 26 ± 0.5 °C with lid on until sampling. Exposed ZFE and controls were sampled at 12, 24, 72, 96 and 120 hpf, each sample containing the pooled ZFE from a single well (n = 9–12). Water samples of 1 ml were taken at the same times from the corresponding well. At sampling, ZFE were washed three times in distilled water and then the liquid was removed by pipetting and samples were stored at −20 °C for analysis. All samples were done in quadruplicate. Further details on experimental conditions as well as picture of embryos at each time points are presented in SI Section S1 Figs. S1–S5.

2.2. Chemical analysis

Samples were analyzed using LC-MS/MS with detailed analysis described in SI section S2 and Tables S1–S3. All measured concentrations in ZFE were expressed in nmol/embryo. The measured water and ZFE concentration in each sample are given in Tables S4–S6 and Figs. S6–S7. Compound amounts were compared at different time points using ANOVA and Tukey's HSD test in R version 4.1.2 (2021-11-01).

2.3. Literature data

A literature search was performed for internal concentrations of environmentally relevant bisphenols selected previously (Chelcea et al., 2022) measured in ZFE at any time between 0 and 168 hpf. Data were collected for BPA (Gibert et al., 2011; Moreman et al., 2017, 2018; Wu et al., 2017; Souder and Gorelick, 2018; Brown et al., 2019; Yang et al., 2019; Fu et al., 2020; Kim et al., 2020; Achenbach et al., 2022), BPAF (Moreman et al., 2017), bisphenol S (BPS) (Le Fol and Brion, 2017; Moreman et al., 2017; Zhang et al., 2017; Achenbach et al., 2022), bisphenol F (BPF) (Gibert et al., 2011; Moreman et al., 2017), and TBBPA (Liu et al., 2018; Achenbach et al., 2022). Available numeric values were extracted from tables, otherwise from graphs using WebPlotDigitizer (n.d). Experimental set-up data were collected for each study (Table S7). The mean volume of a ZFE at each specific time point

was used to transform to amount per embryo. Since data by Souder and Gorelick (2018) were measured using scintillation, the predictions are given for the summed parent and metabolite amounts as this method cannot distinguish the two. Experimental data sources and conditions are presented in Table S7.

Data on relevant physiological parameters were also collected from literature and are presented in SI section S10, Tables S8–S13 and Table 1. Chemical specific parameters used for the model are presented in Table S14.

Table 1
Literature data and Bayesian inference-based data for physiological parameters used for model parameterization.

Parameter name	Description	Mean[a]	Reference
t_hatch	Hatching time (hpf)	60	(Kimmel et al., 1995; Carlsson et al., 2013; Song et al., 2014; Mu et al., 2018; Fan et al., 2019)
t_circulation	Starting time for blood circulation (hpf)	36	(Kimmel et al., 1995; Jacob et al., 2002; Malone et al., 2007; Carlsson et al., 2013; Santoso et al., 2019)
kd_y_ref	Yolk consumtion rate (µl/h) reference value at 26 °C	1.4E-02	(Brox et al., 2014; Halbach et al., 2020; Siméon et al., 2020)
kg_e_ref	Embryo growth rate (µl/h) reference value at 26 °C	2.4E-03	(Halbach et al., 2020; Siméon et al., 2020)
ksg_e_ref	Surface area growth rate after epiboly (mm^2/h) reference value at 28.5 °C	1.8E-02	(Kimmel et al., 1995; Hagedorn et al., 1998; Guo et al., 2017)
BW_Fcard_ref	Reference embryo body weight (ng) at 28.25 C and 48–72 hpf	0.13	(Halbach et al., 2020; Siméon et al., 2020)
F_card_ref	Reference cardiac output (µl/h)	2.0	(Jacob et al., 2002; Malone et al., 2007; Iftimia et al., 2008; Kopp et al., 2010; Santoso et al., 2019)
epiboly_rate_ref	Reference rate of epiboly (fraction/h)	0.13	(Kimmel et al., 1995; Hagedorn et al., 1998)
TA	Arrhenius Temperature (Kelvin)	6930	(Billat et al., 2022) based on data from (Kimmel et al., 1995)
SA_Chorion	Chorion surface area (mm^2)	4.8	(Kimmel et al., 1995; Brox et al., 2014; Diogo et al., 2015)
Vchorion_0	Volume of perivitelline space at 0 hpf (µl)	1.3	(Kimmel et al., 1995; Brox et al., 2014; Diogo et al., 2015)
Ve	Volume of embryo at time-point 0 (µl)	8.9E-03	Kimmel et al. (1995)
Vy	Volume of yolk at time-point 0 (µl)	0.20	(Kimmel et al., 1995; Brox et al., 2014; Siméon et al., 2020)
SA_e	Surface area of blastoderm at end of epiboly (mm^2)	1.7	(Kimmel et al., 1995; Hagedorn et al., 1998)
Km	Substrate concentration at half of Vmax (nmol/µl)	6.21E-03	Calibrated using Bayesian inference
fr_yolk	Fraction of cardiac output going to yolk (unitless)	0.85	Calibrated using Bayesian inference
t_metabolism	Starting time for metabolism (hpf)	72	Calibrated using Bayesian inference[b]
Kp_Chorion	Permeability rate to chorion (mm/h)	0.39	Calibrated using Bayesian inference
Kp_Yolk	Permeability rate to yolk (mm/h)	1.20	Calibrated using Bayesian inference
Kp_E	Permeability rate to embryo (mm/h)	0.69	Calibrated using Bayesian inference

[a] Median in the case of Bayesian calibrated parameters.
[b] Literature data exists but varies (Gibert et al., 2011; Christen and Fent, 2014; Brox et al., 2016; Le Fol and Brion, 2017; Achenbach et al., 2022), thus the parameter was calibrated.

2.4. ZFE model

The toxicokinetic model consists of five compartments before and four after hatching including water, plastic, yolk, embryo and chorion (Fig. 1). The chorion compartment was modelled to represent all membranes of the chorion as well as the perivitelline space and fluid, as done previously (Warner et al., 2022). The chorion compartment was removed in the modelling after hatching, set at 60 hpf. If the literature studies included internal concentrations from dechorionated embryos, then the hatching time for predictions was set to 0.

In early development, the embryo and yolk compartments were modelled to be in direct contact with each other and the chorion compartment (Fig. 1). The embryo was then modelled to dynamically cover the surface area of the yolk over time, thus simulating the biological process of epiboly where the embryonic cells envelop the surface of the yolk early in the development (Fig. 1) (Kimmel et al., 1995; Hagedorn et al., 1997, 1998). When 100% epiboly is reached, at around 10 hpf depending on temperature, the yolk is in direct contact with the embryo body, and not with chorion or water compartments. The epiboly was modelled as a linear rate based on percentage of epiboly as provided by Kimmel et al. (1995) (Table S8).

Diffusion across membranes is believed to be the main driver for chemical exchange (Rombough, 2002; Kämmer et al., 2022). Therefore, flow of chemical into and out of different compartments was modelled using diffusion and permeability equations. The flux of compounds across the ZFE membranes was modelled based on Fick's law of diffusion and is referred to as "permeability-limited" in this study. This process is dependent on the surface area (mm^2) and the concentration gradient between two compartments as well as a permeability rate constant (K_p) (Eq (1)). K_p summarizes both parameters related to membrane permeation including membrane thickness and the diffusivity of specific compounds across membrane due to limited data availability to distinguish those parameters. Similar approaches have been used to model compound movement into ZFE (Warner et al., 2022), dermal absorption in adult fish (Nichols et al., 1996), and uptake in cells *in vitro* (Stadnicka-Michalak et al., 2014). The general compartment equations for flow of compound across membranes were then described as done previously (Nichols et al., 1996) for fish skin diffusion but with the concentration being expressed in terms of amounts and volumes according to;

$$\frac{dA_{c1}}{dt} = K_{pc1:c2} * SA_{c1:c2} * \left(A_{c2} \Big/ V_{c2} - \frac{A_{c1}/V_{c1}}{P_{c1:c2}} \right) \quad (1)$$

where dA_{C1}/dt describes the rate of change in compound amount (nmol/h) in respective compartment 1 (i.e. chorion, embryo, yolk, water). $K_{pc1:c2}$ is the permeability rate constant (mm/h) between compartments 1 and 2, $SA_{c1:c2}$ (mm^2) is the contact surface area between compartments 1 and 2, A is amount (nmol) and V volumes (µl) of the compartments and $P_{c1:c2}$ (unitless) represents the partition coefficient between compartment 1 and 2. In this model, we assumed that K_p remains constant throughout the exposure period.

Volumes of yolk and embryo were modelled to decrease and increase, respectively, over time. Data on yolk and embryo body volume changes (Brox et al., 2014; Guo et al., 2017; Halbach et al., 2020; Siméon et al., 2020) were used to fit the yolk consumption rate as an exponential decay curve (Table S10, Fig. S8), and the embryo growth rate as a linear curve (Table S11, Fig. S9). Mean embryo growth rate (kg_e) and yolk consumption rate (kd_y) are given in Table 1. Volume of the chorion compartment was modelled as the difference between the initial chorion volume and the volumes of yolk and embryo combined (Kimmel et al., 1995; Brox et al., 2014; Diogo et al., 2015). The yolk is assumed a perfect

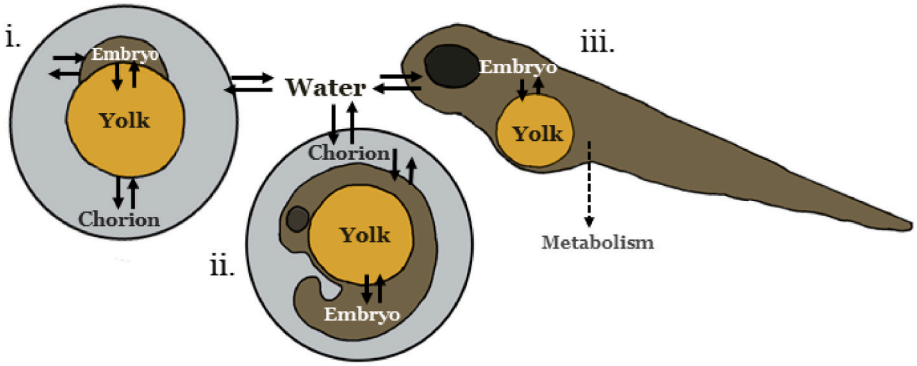

Fig. 1. Structure of the TK model represented for three developmental stages: i) between 0% until 100% epiboly (around 10 hpf) ii) between around 10 hpf until hatching (60 hpf), and iii) > 60 hpf hatching. Arrows represent mass flow of compound between compartments.

sphere with the corresponding surface area calculated based on volume. The embryo surface area in contact with yolk is calculated assuming a hemisphere, that follows a dynamic growth rate equal to the epiboly rate until 100% epiboly. After 100% epiboly, embryo surface area growth was calculated as a linear fit model using measured data on surface area at 100% epiboly (Kimmel et al., 1995; Hagedorn et al., 1998) and at 72, 96 and 120 hpf (Guo et al., 2017) (Table S12). The surface area of the chorion is assumed to be constant as done in previous model (Warner et al., 2022) and calculated based on radius, assuming a perfect sphere (Kimmel et al., 1995; Brox et al., 2014; Diogo et al., 2015). All rates (embryo growth, surface area growth, epiboly, yolk consumption and cardiac output) were adjusted for temperature dependency using the Arrhenius temperature equation (Barron et al., 1987) as done in the adult fish TKs model (See SI section S7) (Grech et al., 2019; Billat et al., 2022; Chelcea et al., 2022). The reference temperatures and rates are presented in Table 1.

Distribution of compound between embryo and yolk was modelled via blood perfusion and partitioning in addition to permeability presented above, starting at >36 hpf. This was described assuming the embryo is a single, homogenous compartment with the blood having the same concentration of compound as in embryo and the flow rate being a fraction of the cardiac output. Equations are given in SI sections S8-S9.

Plastic binding of compound was added as an instant equilibrium process using a previous linear model (Kramer, 2010). This process was only included in the prediction if no measured water concentrations were available and plastic wells were used for experimental set-up. Otherwise, if measured water concentration were available, as for current study, or if glass was used, binding to well walls was set to 0.

Partition coefficients for studied chemicals for yolk-chorion and embryo-chorion were assumed to be the same as for yolk-water and embryo-water, respectively. This simplification was done as the perivitelline space is largely aqueous and the chorion membrane has large pores (Brox et al., 2014). Yolk-water partition ($P_{yolk:water}$) coefficient was predicted using a linear free energy model (LFER) developed previously (Ulrich et al., 2020). The only exception is for BPA, where measured data (Ulrich et al., 2020) was used for the parameterization. Partition coefficients for embryo-water, yolk-embryo and chorion-water, were calibrated for BPZ and then adjusted with the value of the octanol-water partition coefficient (log K_{ow}) (Table S14). This assumes that the partition between these tissues is linearly correlated with the log K_{ow} value of each compound. This was done to enable extrapolation between structurally similar compounds and is further discussed in SI section S10.

Metabolic clearance (Met_{Cl}) was assumed to take place in the embryo body, and was described using Michaelis-Menten kinetics according to;

$$Met_{Cl} = \left(\frac{V_{max} * A_{embryo} / V_{embryo}}{K_m + A_{embryo} / V_{embryo}} \right) * met_{on} \quad (2)$$

$$V_{max} = Cl_{sc} * K_m \quad (3)$$

where V_{max} (nmol/h/μl) describes the maximum velocity of the reaction and K_m (nmol/μl) the concentration of substrate at half of V_{max}. V_{max} and K_m are unknown for the various bisphenols in fish, but information on clearance in fish has been measured for bisphenols.(Chelcea et al., 2022) Clearance scaled for embryo body (Cl_{sc}) was therefore considered equal to V_{max}/K_m ratio as suggested previously (Hoer et al., 2022) since the clearance values were measured at concentrations much below K_m i.e. in the linear part of the kinetic process. The met_{on} parameter was calibrated using Bayesian inference and can take the values of 0 or 1 to account for start of metabolism (t_metabolism). Full equations for each model compartment before and after hatching are presented in SI section S9.

2.5. Bayesian inference

Only measured amounts of BPZ in embryos and water from current study were used for model calibration while all other measured data both from literature as well as from current study were used for validation as an external test set. Bayesian inference was used to estimate distributions and median of model parameters for which no literature information was available including permeability constants (K_p) for yolk, embryo and chorion, all partition coefficients except $P_{yolk:water}$, start time of metabolism (t_metabolism), fraction of cardiac output perfusing the yolk (fry_{olk}) and K_m. Bayesian inference was done using the *DeBInfer* package (Boersch-Supan et al., 2017) developed for compatibility with the ode solver package *deSolve* (Soetaert et al., 2010) used for solving the toxicokinetic model. Details on methodology and priori distributions of the Bayesian inference are presented in Section S11 and post-prior distributions can be seen in Figs. S10–S11. Prediction for BPZ credible interval is shown in Fig. S12.

2.6. Model validation

Collected literature data as well as data on BPA and BPAF from current study were used as an external test set and compared with model predictions, using the mean of parameters collected from literature and the median value of the posterior distributions for the Bayesian calibrated parameters. R^2 was calculated for compounds presented in each graph (Fig. 3) and for all compounds combined with exception of BP-2 and BPS which were considered outside applicability domain due to ionization.

Additionally, sensitivity analysis was performed to investigate influential model parameters. All parameters were varied uniformly with ±10% of their mean or median (if calibrated by Bayesian) values. Sobol indices were calculated based on the area under the curve (AUC) for total amount in whole ZFE (embryo body, yolk and chorion) and for total amount in embryo body after 1000 samples, using the soboljansen function. Results are presented in SI section S12, Fig. S13.

2.7. Relative hazard ranking of ER potency

ER activity of the selected bisphenols was determined in the ER-LUC assay using VM7Luc4E2 cells (formerly known as BG1luc4E2) (Rogers and Denison, 2000). Method details are given in SI section S3.

The nominal EC_{50} ($EC_{50,nom}$) values from the *in vitro* testing were converted into corresponding free concentration ($EC_{50,free}$) based values using the Honda model (Honda et al., 2019) which is an updated version of the Armitage model (Armitage et al., 2014) by applying the armitage_eval (n.d) function of the *httk* package (Wambaugh, 2015) in R version 4.1.2 (2021-11-01) run in RStudio (2022.07.1). The used parameters for this conversion are presented in SI section S4. The maximum concentration (C_{max}) in embryo body (i.e. excluding yolk and chorion) was calculated using developed ZFE model assuming an exposure of 10 μM, at 26 °C, in glass, for 10 embryos in 100 ml water, starting at 0 hpf to 120 hpf. This dose is in the range of model calibration data. The C_{max} was selected as a worst-case exposure situation and as a comparison relative bioaccumulation between bisphenols in ZFE. Lastly, a relative hazard ranking was calculated as the ratio between the C_{max} in embryo body and the ER $EC_{50,free}$ with a higher ratio representing a higher relative hazard.

2.8. Software

Model was developed in R version 4.1.2 (2021-11-01), run in RStudio (2022.07.1), and then implemented in KNIME v.4.4.2. The ODE system was solved using *ode* function in the *desolve* (Soetaert et al., 2010) package. *DebInfer* (Boersch-Supan et al., 2017) and *sensitivity* (Iooss et al., 2022) packages were used for Bayesian inference and sensitivity analysis respectively. An example model script parameterized for BPZ is available in SI 2. All model scripts are implemented in a KNIME (n.d) workflow available on Github (https://github.com/ioanachelcea/ZFE_Bisphenols).

3. Results and discussion

3.1. Experimental concentration in ZFE and water

Although measured internal concentrations in ZFE were available in literature for some bisphenols, few studies include multiple time-points necessary for calibrating TK models and little data is available for bisphenols other than BPA. The experimental ZFE measurements obtained in this study (Table S6) therefore provide data necessary for both model calibration (Fig. 2A) and validation (Fig. 2B and C). Data on water concentrations in the ZFE wells and chemical stability are presented in the SI Tables S4-S5. No significant decrease of compound was observed in water between day 0 and 5 for the stability test ($p > 0.05$; ANOVA Tukey's test) suggesting that BPA, BPAF and BPZ are stable over the tested period indicating adsorption to plastic or abiotic transformation are negligible over time (Table S4). No visible deformations or lethality was observed in either exposed or control ZFE (SI section S1).

When calculating the summed total amount of compound detected in both water and embryos (Fig. S7), there is a significant decrease in amount between the first and last measured time-points at 12 and 120 hpf, respectively. The decrease from 12 hpf is significant ($p < 0.05$; ANOVA Tukey's test) already at 24 hpf for BPAF and BPZ and at 72 hpf for BPA (Fig. S7), which is likely caused by biotransformation of the parent compounds, discussed in more detail below. In comparison, a recent study (Achenbach et al., 2022) measured concentration of BPA in ZFE exposed to a similar water concentration and showed internal amounts in the same order of magnitude as current study.

3.2. Toxicokinetic model

A TK model was developed using our experimental data on BPZ for calibration (Fig. 2A) and incorporating the processes of biotransformation and blood circulation in the embryo as well as hatching. Our experimental observations of the time course of internal concentrations of studied BPs suggest that metabolism may be involved in lowering the concentration in embryos (Kühnert et al., 2013; Halbach et al., 2020). Previous studies observed decreases in internal concentrations at time-points after 48–72 hpf for various compounds including bisphenols. Billat et al. (2022) suggested that this is mainly due to volume dilution. Indeed, the sensitivity analysis of current model indicates that metabolism does not affect the AUC of BPZ in whole ZFE (Fig. S13). However, the sensitivity analysis (Fig. S13) for AUC in embryo body shows that parameters of metabolism such as K_m, clearance rate and start of metabolization are among the top ten sensitive parameters, indicating that metabolism may be relevant for understanding dose at target in the embryo body. Additionally, biotransformation has been

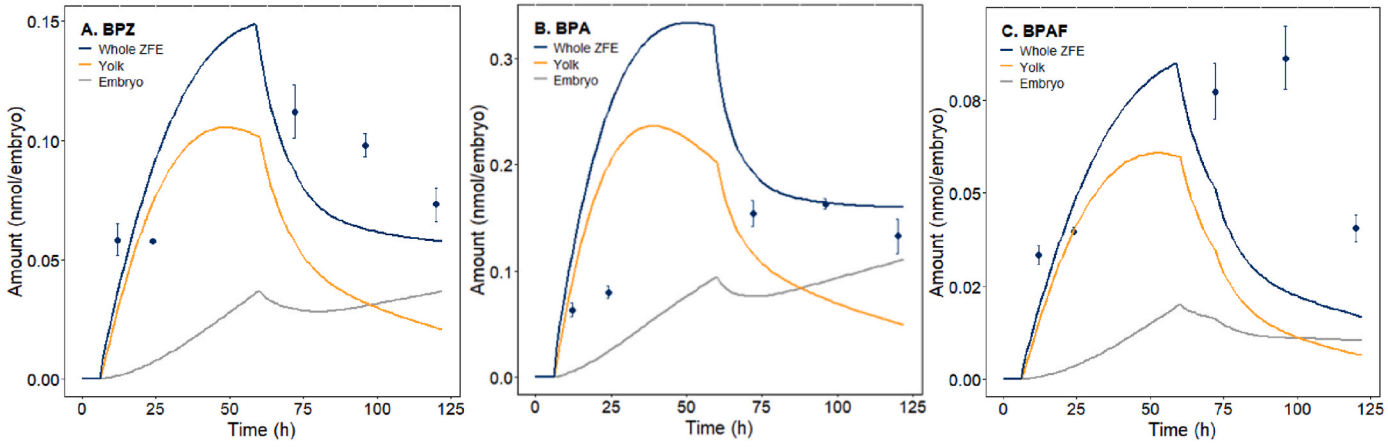

Fig. 2. Model prediction of internal zebrafish embryo (ZFE) amounts compared with measured amounts (dots) for BPZ (A), BPA (B) and BPAF (C) from current study at 4–120 hpf exposure.

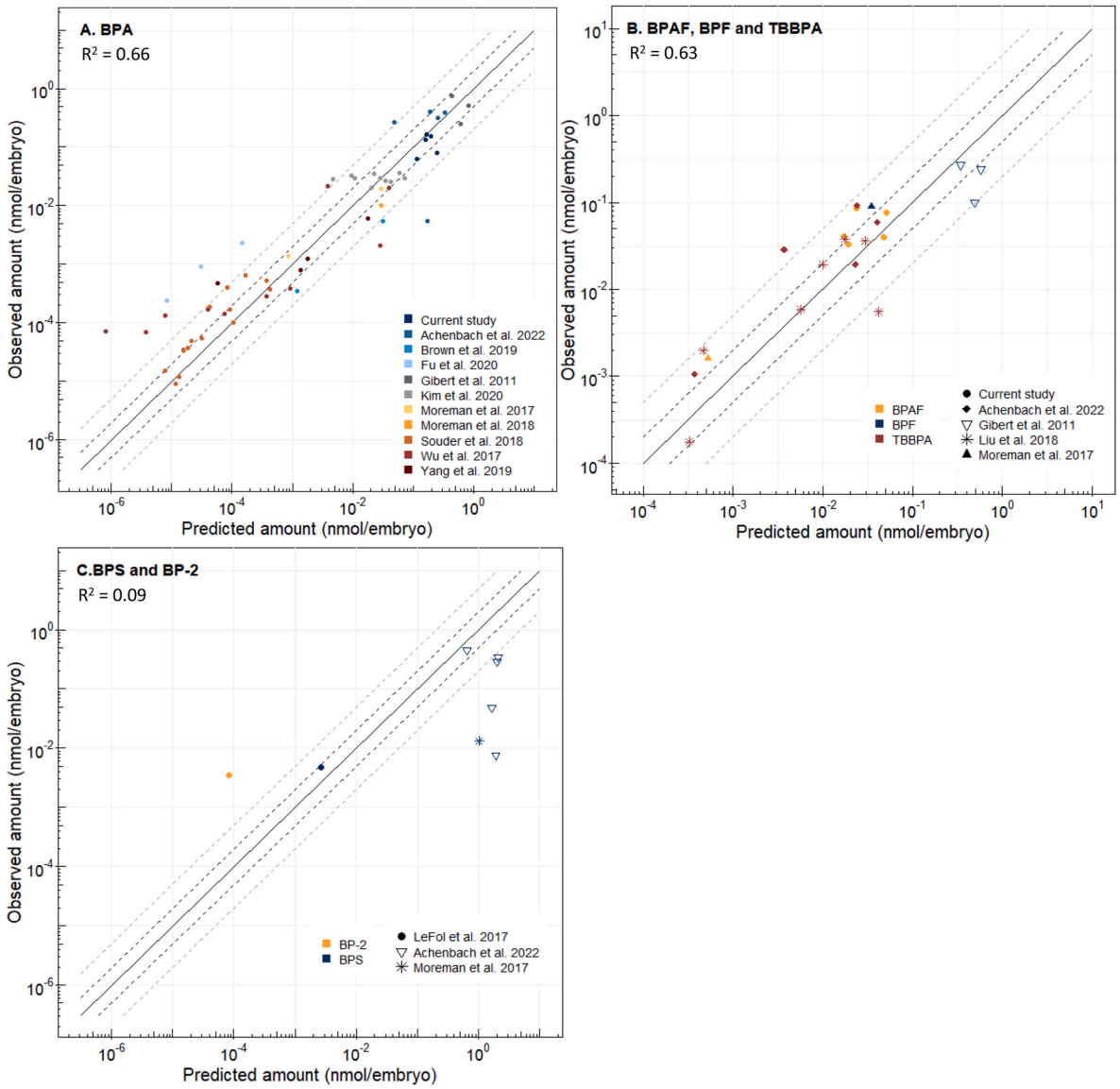

Fig. 3. Observed and predicted amount (nmol) of compound per ZFE (embryo body, yolk and chorion) for BPA (A), BPAF, BPF, TBBPA (B), BPS and BP-2 (C). Solid line represents 1:1 correlation and dotted lines represent the 2-fold (black) and 5-fold- (gray) errors. R^2 was calculated for each graph. Note that all data presented in this Figure was not used in model calibration.

previously documented in ZFE. Several experimental studies (Gibert et al., 2011; Le Fol and Brion, 2017; Achenbach et al., 2022) detected metabolites of BPA, BPS, BP-2, BPF and TBBPA from as early as 6 hpf in ZFE. The posterior distribution for the start of metabolism (t_metabolism) estimates a median of 72 hpf for BPZ (Table 1), which is consistent with literature observations on glucuronidation and sulfation in ZFE (Gibert et al., 2011; Le Fol and Brion, 2017; Achenbach et al., 2022). These biotransformation pathways are believed to be the main processes involved in bisphenol metabolism of vertebrates including fish (Lindholst et al., 2003; Wang et al., 2014; Le Fol and Brion, 2017; Chelcea et al., 2022). Significant increase in expression of glucuronic acid transferases (UGTs) RNA has been observed after 72 hpf in zebrafish embryos (Christen and Fent, 2014). Additionally, glucuronic acid conjugates of BPS, BP2 (Le Fol and Brion, 2017) and BPF (Gibert et al., 2011) have been measured at 72 hpf. A recent study (Achenbach et al., 2022) observed bisphenol glucuronic acid conjugates as early as 6 hpf for BPA and at 20 hpf for BPS and TBBPA, but the levels of metabolites increased drastically only after 48 hpf, suggesting that metabolism may start earlier than 72 hpf but is likely less significant. Glucuronic acid metabolites have also been detected in ZFE for other compounds such as paracetamol or valproic acid, but only after 72 hpf (Brox et al., 2016).

Circulation was added starting at 36 hpf as this is the time point where high flow is observed in the embryo (Table 1) (Kimmel et al., 1995). Despite that blood flow has been observed as early as 24 hpf, it has been shown to be weak with low velocity and heart rate (Jacob et al., 2002; Malone et al., 2007; Carlsson et al., 2013; Santoso et al., 2019). Additionally, heart rate and cardiac output was only measured at 24 hpf when embryos were kept at 31 °C (Jacob et al., 2002), which is close to the tolerable maximum for the species. All reference studies (Jacob et al., 2002; Malone et al., 2007; Carlsson et al., 2013; Santoso et al., 2019), used to sample blood circulation data (Table S13), report heartbeat, blood flow and a measurable cardiac output already at 48 hpf even at temperatures as low as 25 °C, suggesting this process starts between 24 and 48 hpf. Since the yolk is highly perfused (Isogai et al., 2001), and cardiac output is strong after 48 hpf, blood perfusion is likely to influence the transport of compounds between embryo and yolk compartments (Jacob et al., 2002; Malone et al., 2007; Iftimia et al., 2008; Kopp et al., 2010; Santoso et al., 2019). This presents an important physiologically-relevant addition to the ZFE model. The fraction of cardiac output perfusing the yolk (fr_yolk) was estimated with Bayesian

inference at a median value of 0.85 (Table 1) which is consistent with literature data showing high perfusion of the yolk (Isogai et al., 2001).

The role of the chorion as a compound uptake barrier has been previously discussed (Scholz et al., 2008; Henn and Braunbeck, 2011; Brox et al., 2014; Guarin et al., 2021; Billat et al., 2023). Chorion-water partitioning was estimated at a value around one (Table S14), suggesting there is little affinity for the chorion compartment over the water compartment. These findings are consistent with current knowledge on the chorion membrane and perivitelline space (Hisaoka, 1958; Wiegand et al., 2000; Braunbeck et al., 2005; Brox et al., 2014; Guarin et al., 2021). Microscopic images show pores of around 1.5 μm diameter covering the chorion, thus allowing for water and neutral low molecular weight compounds such as bisphenols to pass through (Hisaoka, 1958). Furthermore, studies investigating compound concentration in ZFE before and after dechorination suggest weak barrier function of the chorion itself for low molecular weight compounds (Wiegand et al., 2000; Braunbeck et al., 2005; Brox et al., 2014; Guarin et al., 2021). The chorion may however slow the absorption of ionic or perfluorinated compounds as well as highly lipophilic compounds (Braunbeck et al., 2005; Vogs et al., 2019; Warner et al., 2022; Billat et al., 2023).

3.3. Prediction of internal bisphenol amounts

The calibrated TK model with parameters stated in Table 1 and Table S14 was used to predict uptake and depuration in ZFE of bisphenols (Figs. 2 and 3). For BPA, sampled from 11 different studies including current study (Fig. 2B) at 60 time-points (Fig. 3A), the predictions were within a 5-fold of measured data for 78% of the data points and 48% within 2-fold. The two lowest doses of data by Wu et al. (2017) were vastly under-predicted. However, this study measured highly similar internal embryo concentrations at 168 hpf for ZFE dosed at 100-fold different concentrations (0.004–0.4 μM), which may indicate experimental errors (Wu et al., 2017). Since under-prediction is only observed at low concentrations, saturation of kinetic processes is unlikely to be the explanation but it may be caused by dose-dependent metabolism or uptake processes.

All of the BPAF and BPF data was predicted within a 5-fold error while 50% and 25% were within a 2-fold error, respectively (Fig. 3 B). The model was also capable of predicting kinetics of TBBPA for which 83% of data were within a 5-fold error and 50% within a 2-fold error (Fig. 3B). In contrast, data for BP-2 and BPS was not as accurately predicted with two out of seven data-points for BPS being within a 5-fold error (Fig. 3C) and the single time-point for BP-2 being more than 10-fold different. The acid dissociation rate constant (pKa) for both BPS (pKa = 7.4) and BP-2 (pKa = 2.8) is equal to or below 7.4, previously predicted using Jchem (Chelcea, 2022; Jchem for Office, 2019). Thus, they are partly or largely ionized in the exposure water, a process which is not covered by the developed model and therefore these two bisphenols fall outside its applicability domain. Ionization would likely affect all partition coefficients of these compounds including embryo-water partitioning, which is one of the most sensitive parameters in the model (Fig. S13). A next logical step in the development of our ZFE model would be to adjust for ionizable fraction or apply pH dependent partitioning (log *D*) (Bittner et al., 2019; Siméon et al., 2020).

Overall, the model showed acceptable predictive performance with 84% of all external data points within a 5-fold error and 50% within a 2-fold error. A previous ZFE model for bisphenols (Billat et al., 2022) predicts 63% and 88% of bisphenols data within a 2- and 5-fold error respectively showing somewhat better performance than current model. However, that model was not validated using external data and thus its predictive performance was based on calibration data. A recent ZFE model for perfluorinated compounds (Billat et al., 2023) demonstrated similar performance on external data as current model with 50% of data within a 2-fold error. The accuracy of current model was also considered sufficient, as the experimental outcomes between studies were large, even when experimental design was similar. For example, two studies (Moreman et al., 2017, 2018) using the same experimental set-up with the same measured BPA water concentration, showed a 2-fold difference in mean embryo concentration at 120 hpf. Overall, this shows that the current model is able to predict external data with a large variation of experimental set-up and doses.

Although the model adjusts for start of metabolism, it does not adjust for the fact that embryos may have lower metabolic rates than adults even after scaling for body size. Although a previous study (Le Fol and Brion, 2017) showed that BPS and BP-2 are metabolized to a lesser extent in embryos than adults, there is a general lack of studies comparing metabolic rates between embryo and adult life-stages, making this parameter challenging to estimate. Furthermore, we calibrated the start of metabolism as a single time-point, however, the expression of metabolic enzymes and thus the metabolic capacity increase throughout early development. Thus, a next step in the model development could be to incorporate metabolism as a gradually increasing process to better reflect the physiology.

Currently there is no validation data for bisphenols available for assessing the accuracy of prediction in terms of amount in yolk and embryo separately. The model predicts higher amounts in yolk than in embryo body, which is consistent with data on other compounds such as fluorescent dyes CY3A and TAMRA, as well as carbamazepine, 2-ethylpyridine, 4-iodophenol, diuron and 1,2,4-tribromobenzene, which were measured in both zebrafish embryo and yolk separately (Halbach et al., 2020; Guarin et al., 2021). These compounds have log K_{ow} values ranging from 1.8 to 4.3 which is similar to the log K_{ow} values of the currently investigated bisphenols. The distribution to mostly yolk in early development could in part be due to the high perfusion of the yolk leading to more chemical being transported into this compartment or, more likely, be due to the high protein and fat content of the yolk which can lead to preferential distributions of hydrophobic compounds into this compartment.

A few kinetic models for ZFE have been published in recent years (Kühnert et al., 2013; Brox et al., 2016; Bittner et al., 2019; Vogs et al., 2019; Halbach et al., 2020; Siméon et al., 2020; Billat et al., 2022, 2023; Warner et al., 2022). Most of these models have not been validated on external data and their predictive performance is thus uncertain. Some of the previous models have been tailored for predicting ionic compounds and may therefore be less suited for neutral hydrophobic ones, like most of the bisphenols of current study due to variation in toxicokinetic properties (Bittner et al., 2019; Siméon et al., 2020). Current model is calibrated for neutral bisphenols but it can be developed to include predictive models adjusted for ionization for critical compound specific parameters including partition coefficients. Many ZFE models predict that steady-state of the kinetic processes is reached nearly instantly (Bittner et al., 2019; Halbach et al., 2020; Siméon et al., 2020) which was adjusted in the current model as measured data indicates that steady-state is not reached throughout the 120 h of exposure. Some of previous models have been designed with direct flow from water into yolk (Kühnert et al., 2013; Vogs et al., 2019; Siméon et al., 2020; Billat et al., 2022). This has been changed in current model based on observations that after 100% epiboly the yolk is completely covered by the embryo body (Kimmel et al., 1995; Hagedorn et al., 1997; Kaufmann et al., 2012; Cartner et al., 2019). This means that the compound has to pass through the embryo body before reaching the yolk, which influences the rate of the kinetic processes. In most previous models, fitting of parameters was performed using algorithms which do not consider inter-parameter covariances (Kühnert et al., 2013; Bittner et al., 2019; Vogs et al., 2019). Recently, a model for for bisphenols and one for perfluorinated compounds with dynamic volumes and a Bayesian approach for calibrating parameters have been developed (Billat et al., 2022, 2023), thus presenting improvements to previous models. However, the bisphenol model has not been validated on external data unlike current model.

3.4. Hazard ranking of bisphenols

The hazard of studied bisphenols was ranked relative to each other combining measured *in vitro* ER potency with estimated exposure in terms of internal ZFE concentrations. We determined their estrogenicity using the VM7Luc4E2 cell assay expressing human ERα and ERβ (Table 2) (OECD, 2012). Although the assay expresses human ER as opposed to zebrafish ER, this target is highly conserved across vertebrates (OECD, 2018). A previous study also reported comparable EC_{50} values for ER activation between zebrafish cell lines and other *in vitro* systems (Le Fol and Aït-Aïssa, 2017). The estrogenic potency of the bisphenols spanned between 0.07 μM for BPAF to 2.1 μM for BPAP excluding TBBPA and Bimox M for which no response was recorded (Table 2, $EC_{50,nom}$). The internal exposure in ZFE was estimated as the C_{max} of compound in the embryo body i.e. excluding yolk and chorion, predicted using the developed ZFE model. The body of the embryo is the part of the ZFE that displays expression and activation of ER (Gorelick and Halpern, 2011; Gorelick et al., 2014) and therefore ZFE concentration was considered as the most relevant proxy for dose at target.

We decided to apply $EC_{50,free}$ values rather than nominal for the relative hazard ranking, since previous studies on *in vitro* to ZFE extrapolations has shown that free concentrations *in vitro* is a better proxy for effects in ZFE (Lungu-Mitea et al., 2021) and it has been proposed to be more suitable for *in vitro* to *in vivo* extrapolation (IVIVE) (Henneberger et al., 2021). The relative hazard ranking ($C_{max}/EC_{50,free}$) represents a worst case scenario both in terms of exposure (C_{max}) but also effect ($EC_{50,free}$) since it assumes the free concentration *in vitro* is comparable to the total concentration in embryo. There is some uncertainty related to the *in vitro* to *in vivo* extrapolation, considering free internal cell concentrations and free internal embryo concentrations would be a more suitable comparison as the ER is a nuclear receptor. However, due to limited knowledge regarding the unbound fraction of compound within either cells *in vitro* or ZFE, using the free medium concentration and the total ZFE concentration still provides a closer indication of dose at target than the use of nominal concentrations. The ratio indicates that BPAF followed by BPC, BPB and BPZ are of greater concern than BPA (Table 2). BPAF has the highest measured potency but also reaches the target at highest level. The major difference in hazard ranking was observed between BPA and BPZ, where $EC_{50,nom}$ suggests that BPA may be more hazardous than BPZ, while taking into account free concentration as well as dose at target indicate otherwise.

The relative hazard ranking ratio was then compared with data on lowest observed effect concentration (LOEC) for vitellogenin 1 (*vtg1)* induction in ZFE of various bisphenols (Muncke and Eggen, 2006; Wang et al., 2011; Mu et al., 2018; Gao et al., 2022). Increased levels of vitellogenin is a key event in an AOP under development with ER agonism as MIE and reproductive dysfunction as adverse outcome and it is a commonly used biomarker for estrogenicity (Ankley, 2010; AOP-Wiki,). The literature data on *vtg1* (Muncke and Eggen, 2006; Wang et al., 2011; Mu et al., 2018; Gao et al., 2022) showed similar trend as our hazard ranking with BPAF being most potent followed by BPB showing induction at lower concentrations than BPA. Compiled data indicates that BPC do not follow this trend which may be due to that BPC also can display antagonistic estrogen activity on ERα (Pinto et al., 2019). Furthermore, it has been shown that ER activation varies between bisphenols related to forms of ER in zebrafish with BPA having a higher selectivity for zebrafish ERα, while BPF showed higher selectivity for ERβ2 and BPS for ERβ1 (Le Fol and Aït-Aïssa, 2017). The *vtg1* data also indicates that bisphenols indeed reach the target as predicted by the ZFE model and cause a measurable effect.

Table 2
Relative hazard ranking of bisphenols based on estrogenic potency and C_{max} in ZFE compared to vtg1 data.

Compound	$EC_{50,nom}$ (μM)[a]	$EC_{50,free}$ (μM)[b]	C_{max} (μM)[c]	Relative hazard ranking[d]	LOEC[e] for *vtg1* induction (μM)	Reference for LOEC
BPAF	0.07	0.02	0.52	23	0.77	(Mu et al., 2018; Gao et al., 2022)
BPC	0.13	0.05	0.47	9.8	>3.9[f]	Gao et al. (2022)
BPB	0.17	0.07	0.41	5.5	0.83	Gao et al. (2022)
BPZ	0.30	0.09	0.47	5.4		
BPA	0.26	0.16	0.32	1.9	5.99	(Muncke and Eggen, 2006; Wang et al., 2011; Mu et al., 2018; Gao et al., 2022)
BPF	0.58	0.45	0.23	0.51	8.12	(Mu et al., 2018; Gao et al., 2022)
BPAP	2.1	0.97	0.49	0.50	>1.72[f]	Gao et al. (2022)

[a] Nominal EC_{50} determined in current study.
[b] Free concentration in cell media predicted using a model by Honda et al. (2019) at nominal EC_{50}, with assay specific parameters provided in SI Section S4.
[c] Predicted embryo body (i.e. excluding chorion and yolk) maximal concentration using developed ZFE model at 10 μM hypothetical exposure.
[d] Calculated as $C_{max}/EC_{50,free}$.
[e] Mean of lowest observed effect concentration in ZFE taken from references given in table.
[f] No effect observed, thus the highest tested concentration is given.

4. Conclusions

The current model predicts a wide range of exposure scenarios, including different temperatures, solvent concentrations, various exposure starts and durations as well as compound concentrations ranging from as low as 0.45 nM (Wu et al., 2017) to as high as 50 μM (Gibert et al., 2011). This shows that the model is able to predict in the range of environmentally relevant water concentrations of 1–91 nM reported for BPA (Belfroid et al., 2002; Crain et al., 2007; Chen et al., 2016) and BPAF (Chen et al., 2016).

A challenge in evaluation of the presented model was variability of experimental conditions among ZFE studies found in literature. Evaluation of the 14 studies considered, revealed both differences across and within the same laboratory (Table S7). Variability in measured internal concentrations between studies using similar doses and experimental conditions was comparable to the accuracy of the predicted internal concentrations, namely 2 to 10-fold. Such results highlights that the proposed approach could account for differences in experimental approaches between *in vitro* studies. Additionally, the presented ZFE model can provide a systematic approach to facilitate a key regulatory challenge – comparison and evaluation of ZFE evidence conducted under heterogeneous experimental exposure regimes, conditions and exposure windows. By adjusting for environmental condition differences, the predicted internal concentrations in ZFE can be used to compare studies more accurately and thus better inform weight of evidence approaches for future assessment of chemical risk. Applying this model to estimate internal concentrations could explain some of the heterogeneity in toxicity findings and bioconcentration factors between various ZFE studies. Additionally, it can also address to what extent observed toxicity is affected by accumulation rather than intrinsic potency as previously discussed for PFASs (Vogs et al., 2019). Considering predicted internal ZFE concentrations, rather than nominal ones could aid in establishing more homogenous dose-response relationships based on multiple studies. This in turn would make the model a useful tool for *in vitro* to *in vivo* extrapolation and help derive safety limits for regulatory purpose.

Although ZFE toxicity testing mainly has implications for

environmental safety, as an alternative to adult fish, it has also been employed for understanding pathologies in vertebrates including humans (Veldman and Lin, 2008). Additionally, ZFE test has been suggested in the OECD guideline 250 as a way to identify endocrine disrupting compounds (OECD, 2021). As such, the presented ZFE model, which incorporates critical physiological changes, may prove to be a useful tool for better understanding effects and sensitive windows of development in vertebrates including humans, as it would improve the accuracy of extrapolations across species. Future development should focus on inclusion of ionization and more accurate biotransformation rate parameterization that would improve model predictions.

CRediT authorship contribution statement

Ioana Chelcea: Conceptualization, Methodology, Software, Formal analysis, Data curation, Investigation, Visualization, Writing – original draft. **Carolina Vogs:** Conceptualization, Supervision, Writing – review & editing. **Timo Hamers:** Conceptualization, Supervision, Writing – review & editing, Funding acquisition. **Jacco Koekkoek:** Investigation, Writing – review & editing. **Jessica Legradi:** Conceptualization, Investigation, Supervision, Writing – review & editing. **Maria Sapounidou:** Conceptualization, Supervision, Writing – review & editing. **Stefan Örn:** Conceptualization, Supervision, Writing – review & editing, Funding acquisition. **Patrik L. Andersson:** Project administration, Conceptualization, Supervision, Writing – review & editing, Funding acquisition.

Declaration of competing interest

The authors declare that they have no known competing financial interests or personal relationships that could have appeared to influence the work reported in this paper.

Data availability

Example code for BPZ has been shared in SI_2. Full workflow will be made publicly accessible on GitHub after revision process.

Acknowledgements

We acknowledge Peter Cenijn (VU, Amsterdam) for his help with the ZFE experimental work and the chemical stability testing. The research was financially supported by the Swedish Research Council, grant no. 2019-01838 and no. 2017-01036 and the Kempe foundation.

Appendix A. Supplementary data

Supplementary data to this article can be found online at https://doi.org/10.1016/j.chemosphere.2023.140399.

References

Achenbach, J.C., et al., 2022. Evaluation of the uptake, metabolism, and secretion of toxicants by zebrafish larvae. Toxicol. Sci. https://doi.org/10.1093/toxsci/kfac102 kfac102. Available at:

Ankley, G.T., et al., 2010. Adverse outcome pathways: a conceptual framework to support ecotoxicology research and risk assessment. Environ. Toxicol. Chem. 29 (3), 730–741. https://doi.org/10.1002/etc.34.

AOP-Wiki (no date) . Available at: https://aopwiki.org/aops/29 (Accessed: 19 December 2022).

armitage_eval: Evaluate the updated Armitage model in httk: High-Throughput Toxicokinetics (no date). Available at: https://rdrr.io/cran/httk/man/armitage_eval.html (Accessed: 8 December 2022).

Armitage, J.M., Wania, F., Arnot, J.A., 2014. Application of mass balance models and the chemical activity concept to facilitate the use of in vitro toxicity data for risk assessment. Environ. Sci. Technol. 48 (16), 9770–9779. https://doi.org/10.1021/es501955g.

Barron, M.G., Tarr, B.D., Hayton, W.L., 1987. Temperature-dependence of cardiac output and regional blood flow in rainbow trout, Salmo gairdneri Richardson. J. Fish. Biol. 31 (6), 735–744. https://doi.org/10.1111/j.1095-8649.1987.tb05276.x.

Belfroid, A., et al., 2002. Occurrence of bisphenol A in surface water and uptake in fish: evaluation of field measurements. Chemosphere 49 (1), 97–103. https://doi.org/10.1016/S0045-6535(02)00157-1.

Billat, P.-A., et al., 2022. 'A PBPK model to evaluate zebrafish eleutheroembryos' actual exposure: bisphenol A and analogs' (AF, F, and S) case studies', *Environmental Science and Pollution Research* [Preprint]. https://doi.org/10.1007/s11356-022-22741-2.

Billat, P.-A., et al., 2023. PBTK modeled perfluoroalkyl acid kinetics in zebrafish eleutheroembryos suggests impacts on bioconcentrations by chorion porosity dynamics. Toxicol. Vitro 89, 105588. https://doi.org/10.1016/j.tiv.2023.105588.

Bittner, L., et al., 2019. Combined ion-trapping and mass balance models to describe the pH-dependent uptake and toxicity of acidic and basic pharmaceuticals in zebrafish embryos (Danio rerio). Environ. Sci. Technol. 53 (13), 7877–7886. https://doi.org/10.1021/acs.est.9b02563.

Boersch-Supan, P.H., Ryan, S.J., Johnson, L.R., 2017. deBInfer: Bayesian inference for dynamical models of biological systems in R. Methods Ecol. Evol. 8 (4), 511–518. https://doi.org/10.1111/2041-210X.12679.

Braunbeck, T., et al., 2005. Towards an alternative for the acute fish LC50 test in chemical assessment: the fish embryo toxicity test goes multi-species - an update. ALTEX - Alternatives to animal experimentation 22 (2), 87–102.

Brown, A.R., et al., 2019. Cardiovascular effects and molecular mechanisms of bisphenol A and its metabolite MBP in zebrafish. Environ. Sci. Technol. 53 (1), 463–474. https://doi.org/10.1021/acs.est.8b04281.

Brox, S., et al., 2014. Influence of the perivitelline space on the quantification of internal concentrations of chemicals in eggs of zebrafish embryos (Danio rerio). Aquat. Toxicol. 157, 134–140. https://doi.org/10.1016/j.aquatox.2014.10.008.

Brox, S., et al., 2016. Toxicokinetics of polar chemicals in zebrafish embryo (Danio rerio): influence of physicochemical properties and of biological processes. Environ. Sci. Technol. 50 (18), 10264–10272. https://doi.org/10.1021/acs.est.6b04325.

Carlsson, G., et al., 2013. Toxicity of 15 veterinary pharmaceuticals in zebrafish (Danio rerio) embryos. Aquat. Toxicol. 126, 30–41. https://doi.org/10.1016/j.aquatox.2012.10.008.

Cartner, S., et al., 2019. The Zebrafish in Biomedical Research: Biology, Husbandry, Diseases, and Research Applications. Academic Press.

Chelcea, I., et al., 2022. Physiologically based toxicokinetic modeling of bisphenols in zebrafish (Danio rerio) accounting for variations in metabolic rates, brain distribution, and liver accumulation. Environ. Sci. Technol. 56 (14), 10216–10228. https://doi.org/10.1021/acs.est.2c01292.

Chen, D., et al., 2016. Bisphenol analogues other than BPA: environmental occurrence, human exposure, and toxicity—a review. Environ. Sci. Technol. 50 (11), 5438–5453. https://doi.org/10.1021/acs.est.5b05387.

Christen, V., Fent, K., 2014. Tissue-, sex- and development-specific transcription profiles of eight UDP-glucuronosyltransferase genes in zebrafish (Danio rerio) and their regulation by activator of aryl hydrocarbon receptor. Aquat. Toxicol. 150, 93–102. https://doi.org/10.1016/j.aquatox.2014.02.019.

Crain, D.A., et al., 2007. An ecological assessment of bisphenol-A: evidence from comparative biology. Reprod. Toxicol. 24 (2), 225–239. https://doi.org/10.1016/j.reprotox.2007.05.008.

Diogo, P., et al., 2015. Assessment of nutritional supplementation in phospholipids on the reproductive performance of zebrafish, Danio rerio (Hamilton, 1822). J. Appl. Ichthyol. 31 (S1), 3–9. https://doi.org/10.1111/jai.12733.

d'Amora, M., Giordani, S., 2018. 'The utility of zebrafish as a model for screening developmental neurotoxicity'. Front. Neurosci., 12. Available at: https://www.frontiersin.org/articles/10.3389/fnins.2018.00976. (Accessed 6 December 2022). :

Escher, B.I., Hermens, J.L.M., 2002. Modes of action in ecotoxicology: their role in body burdens, species sensitivity, QSARs, and mixture effects. Environ. Sci. Technol. 36 (20), 4201–4217. https://doi.org/10.1021/es015848h.

Fan, X., et al., 2019. Starvation Stress Affects the Maternal Development and Larval Fitness in Zebrafish (Danio rerio), vol. 695. Science of The Total Environment, 133897. https://doi.org/10.1016/j.scitotenv.2019.133897.

Fu, J., et al., 2020. Nano-TiO2 Enhanced Bioaccumulation and Developmental Neurotoxicity of Bisphenol a in Zebrafish Larvae, vol. 187. Environmental Research, 109682. https://doi.org/10.1016/j.envres.2020.109682.

Gao, Y., et al., 2022. Assessing the toxicity of bisphenol A and its six alternatives on zebrafish embryo/larvae. Aquat. Toxicol. 246, 106154 https://doi.org/10.1016/j.aquatox.2022.106154.

Gibert, Y., et al., 2011. Bisphenol A induces otolith malformations during vertebrate embryogenesis. BMC Dev. Biol. 11 (1), 4. https://doi.org/10.1186/1471-213X-11-4.

Gorelick, D.A., Halpern, M.E., 2011. Visualization of estrogen receptor transcriptional activation in zebrafish. Endocrinology 152 (7), 2690–2703. https://doi.org/10.1210/en.2010-1257.

Gorelick, D.A., et al., 2014. Transgenic zebrafish reveal tissue-specific differences in estrogen signaling in response to environmental water samples. Environ. Health Perspect. 122 (4), 356–362. https://doi.org/10.1289/ehp.1307329.

Grech, A., et al., 2019. Generic physiologically-based toxicokinetic modelling for fish: integration of environmental factors and species variability. Sci. Total Environ. 651 (Pt 1), 516–531. https://doi.org/10.1016/j.scitotenv.2018.09.163.

Guarin, M., et al., 2021. Pharmacokinetics in zebrafish embryos (ZFE) following immersion and intrayolk administration: a fluorescence-based analysis. Pharmaceuticals 14 (6), 576. https://doi.org/10.3390/ph14060576.

Guo, Y., et al., 2017. Three-dimensional reconstruction and measurements of zebrafish larvae from high-throughput axial-view in vivo imaging. Biomed. Opt Express 8 (5), 2611–2634. https://doi.org/10.1364/BOE.8.002611.

Hagedorn, M., et al., 1997. Water distribution and permeability of zebrafish embryos, Brachydanio rerio. J. Exp. Zool. 278 (6), 356–371, 10.1002/(SICI)1097-010X(19970815)278:6<356::AID-JEZ3>3.0.CO;2-N.

Hagedorn, M., et al., 1998. Characterization of a major permeability barrier in the zebrafish Embryo1. Biol. Reprod. 59 (5), 1240–1250. https://doi.org/10.1095/biolreprod59.5.1240.
Halbach, K., et al., 2020. Yolk sac of zebrafish embryos as backpack for chemicals? Environ. Sci. Technol. 54 (16), 10159–10169. https://doi.org/10.1021/acs.est.0c02068.
Henn, K., Braunbeck, T., 2011. Dechorionation as a tool to improve the fish embryo toxicity test (FET) with the zebrafish (Danio rerio). Comp. Biochem. Physiol. C Toxicol. Pharmacol. 153 (1), 91–98. https://doi.org/10.1016/j.cbpc.2010.09.003.
Henneberger, L., et al., 2021. Quantitative in vitro-to-in vivo extrapolation: nominal versus freely dissolved concentration. Chem. Res. Toxicol. 34 (4), 1175–1182. https://doi.org/10.1021/acs.chemrestox.1c00037.
Hisaoka, K.K., 1958. Microscopic studies of the teleost chorion. Trans. Am. Microsc. Soc. 77 (3), 240–243. https://doi.org/10.2307/3223685.
Hoer, D., et al., 2022. Predicting nonlinear relationships between external and internal concentrations with physiologically based pharmacokinetic modeling. Toxicol. Appl. Pharmacol. 440, 115922 https://doi.org/10.1016/j.taap.2022.115922.
Honda, G.S., et al., 2019. Using the concordance of in vitro and in vivo data to evaluate extrapolation assumptions. PLoS One 14 (5), e0217564. https://doi.org/10.1371/journal.pone.0217564.
Iftimia, N.V., et al., 2008. Dual-beam Fourier domain optical Doppler tomography of zebrafish. Opt Express 16 (18), 13624–13636. https://doi.org/10.1364/OE.16.013624.
Iooss, B., et al., 2022. Sensitivity: global sensitivity analysis of model outputs. https://CRAN.R-project.org/package=sensitivity. (Accessed 13 December 2022).
Isogai, S., Horiguchi, M., Weinstein, B.M., 2001. The vascular anatomy of the developing zebrafish: an atlas of embryonic and early larval development. Dev. Biol. 230 (2), 278–301. https://doi.org/10.1006/dbio.2000.9995.
Jacob, E., et al., 2002. Influence of hypoxia and of hypoxemia on the development of cardiac activity in zebrafish larvae. Am. J. Physiol. Regul. Integr. Comp. Physiol. 283 (4), R911–R917. https://doi.org/10.1152/ajpregu.00673.2001.
Jchem for Office, 2019. Chemaxon. https://chemaxon.com/products/jchem-for-office. (Accessed 29 October 2019).
Kämmer, N., Erdinger, L., Braunbeck, T., 2022. The onset of active gill respiration in post-embryonic zebrafish (Danio rerio) larvae triggers an increased sensitivity to neurotoxic compounds. Aquat. Toxicol. 249, 106240 https://doi.org/10.1016/j.aquatox.2022.106240.
Kaufmann, A., et al., 2012. Multilayer mounting enables long-term imaging of zebrafish development in a light sheet microscope. Development 139 (17), 3242–3247. https://doi.org/10.1242/dev.082586.
Kim, S.S., et al., 2020. Neurochemical and behavioral analysis by acute exposure to bisphenol A in zebrafish larvae model. Chemosphere 239, 124751. https://doi.org/10.1016/j.chemosphere.2019.124751.
Kimmel, C.B., et al., 1995. Stages of embryonic development of the zebrafish. Dev. Dynam. 203 (3), 253–310. https://doi.org/10.1002/aja.1002030302.
KNIME - Open for Innovation (no date). Available at: https://www.knime.com/(Accessed: 5 May 2018).
Kopp, R., et al., 2010. Chronic reduction in cardiac output induces hypoxic signaling in larval zebrafish even at a time when convective oxygen transport is not required. Physiol. Genom. 42A (1), 8–23. https://doi.org/10.1152/physiolgenomics.00052.2010.
Kramer, N.I., 2010. Measuring, Modeling, and Increasing the Free Concentration of Test Chemicals in Cell Assays. Dissertation. Utrecht University. https://dspace.library.uu.nl/handle/1874/37545. (Accessed 17 November 2022).
Kühnert, A., et al., 2013. The internal concentration of organic substances in fish embryos—a toxicokinetic approach. Environ. Toxicol. Chem. 32 (8), 1819–1827. https://doi.org/10.1002/etc.2239.
Le Fol, V., Aït-Aïssa, S., 2017. In vitro and in vivo estrogenic activity of BPA, BPF and BPS in zebrafish-specific assays. Ecotoxicol. Environ. Saf. 142, 150–156. https://doi.org/10.1016/j.ecoenv.2017.04.009.
Le Fol, V., Brion, F., 2017. Comparison of the in vivo biotransformation of two emerging estrogenic contaminants, BP2 and BPS, in zebrafish embryos and adults. Int. J. Mol. Sci. 18 (4) https://doi.org/10.3390/ijms18040704.
Lindholst, C., et al., 2003. Metabolism of bisphenol A in zebrafish (Danio rerio) and rainbow trout (Oncorhynchus mykiss) in relation to estrogenic response. Comp. Biochem. Physiol. C Toxicol. Pharmacol. 135 (2), 169–177. https://doi.org/10.1016/S1532-0456(03)00088-7.
Liu, H., et al., 2018. Pharmacokinetics and effects of tetrabromobisphenol a (TBBPA) to early life stages of zebrafish (Danio rerio). Chemosphere 190, 243–252. https://doi.org/10.1016/j.chemosphere.2017.09.137.
Liu, J., et al., 2021. Occurrence, Toxicity and Ecological Risk of Bisphenol A Analogues in Aquatic Environment – A Review, vol. 208. Ecotoxicology and Environmental Safety, 111481. https://doi.org/10.1016/j.ecoenv.2020.111481.
Lungu-Mitea, S., et al., 2021. Modeling bioavailable concentrations in zebrafish cell lines and embryos increases the correlation of toxicity potencies across test systems. Environ. Sci. Technol. 55 (1), 447–457. https://doi.org/10.1021/acs.est.0c04872.
Malone, M.H., et al., 2007. Laser-scanning velocimetry: a confocal microscopy method for quantitative measurement of cardiovascular performance in zebrafish embryos and larvae. BMC Biotechnol. 7 (1), 40. https://doi.org/10.1186/1472-6750-7-40.
Marty, M.S., Carney, E.W., Rowlands, J.C., 2011. Endocrine disruption: historical perspectives and its impact on the future of toxicology testing. Toxicol. Sci. 120 (Suppl. l_1), S93–S108. https://doi.org/10.1093/toxsci/kfq329.
Moreman, J., et al., 2017. Acute toxicity, teratogenic, and estrogenic effects of bisphenol A and its alternative replacements bisphenol S, bisphenol F, and bisphenol AF in zebrafish embryo-larvae. Environ. Sci. Technol. 51 (21), 12796–12805. https://doi.org/10.1021/acs.est.7b03283.
Moreman, J., et al., 2018. Estrogenic mechanisms and cardiac responses following early life exposure to bisphenol A (BPA) and its metabolite 4-Methyl-2,4-bis(p-hydroxyphenyl)pent-1-ene (MBP) in zebrafish. Environ. Sci. Technol. 52 (11), 6656–6665. https://doi.org/10.1021/acs.est.8b01095.
Mu, X., et al., 2018. Developmental effects and estrogenicity of bisphenol A alternatives in a zebrafish embryo model. Environ. Sci. Technol. 52 (5), 3222–3231. https://doi.org/10.1021/acs.est.7b06255.
Muncke, J., Eggen, R.I.L., 2006. Vitellogenin 1 mRNA as an early molecular biomarker for endocrine disruption in developing zebrafish (Danio rerio). Environ. Toxicol. Chem. 25 (10), 2734–2741. https://doi.org/10.1897/05-683R.1.
Nichols, J.W., et al., 1996. A physiologically based toxicokinetic model for dermal absorption of organic chemicals by fish. Fund. Appl. Toxicol. 31 (2), 229–242. https://doi.org/10.1006/faat.1996.0095.
OECD, 2012. Test No. 455: Performance-Based Test Guideline for Stably Transfected Transactivation in Vitro Assays to Detect Estrogen Receptor Agonists. Organisation for Economic Co-operation and Development, Paris. https://www.oecd-ilibrary.org/environment/test-no-455-performance-based-test-guideline-for-stably-transfected-transactivation-in-vitro-assays-to-detect-estrogen-receptor-agonists_9789264185388-en. (Accessed 18 November 2022).
OECD, 2018. OECD in Vitro Screens (Conceptual Framework Level 2). OCDE, Paris, pp. 99–157. https://doi.org/10.1787/9789264304741-4-en.
OECD, 2021. Test No. 250: EASZY Assay - Detection of Endocrine Active Substances, Acting through Estrogen Receptors, Using Transgenic tg(cyp19a1b:GFP) Zebrafish embrYos. Organisation for Economic Co-operation and Development, Paris. https://www.oecd-ilibrary.org/environment/test-no-250-easzy-assay-detection-of-endocrine-active-substances-acting-through-estrogen-receptors-using-transgenic-tg-cyp19a1b-gfp-zebrafish-embryos_0a39b48b-en. (Accessed 25 July 2023).
Pinto, C., et al., 2019. Differential activity of BPA, BPAF and BPC on zebrafish estrogen receptors in vitro and in vivo. Toxicol. Appl. Pharmacol. 380, 114709 https://doi.org/10.1016/j.taap.2019.114709.
Punt, A., et al., 2020. New approach methodologies (NAMs) for human-relevant biokinetics predictions: meeting the paradigm shift in toxicology towards an animal-free chemical risk assessment. ALTEX - Alternatives to animal experimentation 37 (4), 607–622. https://doi.org/10.14573/altex.2003242.
Rogers, J.M., Denison, M.S., 2000. Recombinant cell bioassays for endocrine disruptors: development of a stably transfected human ovarian cell line for the detection of estrogenic and anti-estrogenic chemicals. Vitro Mol. Toxicol. 13 (1), 67–82.
Rombough, P., 2002. Gills are needed for ionoregulation before they are needed for O2 uptake in developing zebrafish, Danio rerio. J. Exp. Biol. 205 (12), 1787–1794. https://doi.org/10.1242/jeb.205.12.1787.
Santoso, F., et al., 2019. Development of a simple ImageJ-based method for dynamic blood flow tracking in zebrafish embryos and its application in drug toxicity evaluation. Inventions 4 (4), 65. https://doi.org/10.3390/inventions4040065.
Scholz, S., et al., 2008. The zebrafish embryo model in environmental risk assessment—applications beyond acute toxicity testing. Environ. Sci. Pollut. Control Ser. 15 (5), 394–404. https://doi.org/10.1007/s11356-008-0018-z.
Segner, H., 2009. Zebrafish (Danio rerio) as a model organism for investigating endocrine disruption. Comp. Biochem. Physiol. C Toxicol. Pharmacol. 149 (2), 187–195. https://doi.org/10.1016/j.cbpc.2008.10.099.
Siméon, S., et al., 2020. Development of a generic zebrafish embryo PBPK model and application to the developmental toxicity assessment of valproic acid analogs. Reprod. Toxicol. 93, 219–229. https://doi.org/10.1016/j.reprotox.2020.02.010.
Soetaert, K., Petzoldt, T., Setzer, R.W., 2010. Solving differential equations in R: package deSolve. J. Stat. Software 33, 1–25. https://doi.org/10.18637/jss.v033.i09.
Song, M., et al., 2014. Assessing developmental toxicity and estrogenic activity of halogenated bisphenol A on zebrafish (Danio rerio). Chemosphere 112, 275–281. https://doi.org/10.1016/j.chemosphere.2014.04.084.
Souder, J.P., Gorelick, D.A., 2018. Assaying uptake of endocrine disruptor compounds in zebrafish embryos and larvae. Comparative biochemistry and physiology. Toxicology & pharmacology: CBP 208, 105–113. https://doi.org/10.1016/j.cbpc.2017.09.007.
Stadnicka-Michalak, J., et al., 2014. Measured and modeled toxicokinetics in cultured fish cells and application to in vitro - in vivo toxicity extrapolation. PLoS One 9 (3), e92303. https://doi.org/10.1371/journal.pone.0092303.
Tišler, T., et al., 2016. Hazard identification and risk characterization of bisphenols A, F and AF to aquatic organisms. Environ. Pollut. 212, 472–479. https://doi.org/10.1016/j.envpol.2016.02.045.
Ulrich, N., et al., 2020. Yolk–water partitioning of neutral organic compounds in the model organism Danio rerio. Environ. Toxicol. Chem. 39 (8), 1506–1516. https://doi.org/10.1002/etc.4744.
Veldman, M.B., Lin, S., 2008. Zebrafish as a developmental model organism for pediatric research. Pediatr. Res. 64 (5), 470–476. https://doi.org/10.1203/PDR.0b013e318186e609.
Vogs, C., et al., 2019. Toxicokinetics of perfluorinated alkyl acids influences their toxic potency in the zebrafish embryo (Danio rerio). Environ. Sci. Technol. 53 (7), 3898–3907. https://doi.org/10.1021/acs.est.8b07188.
Wambaugh, J., 2015. *High-throughput toxicokinetics (HTTK) R package*. CompTox CoP presentation, US EPA. https://cfpub.epa.gov/si/si_public_record_report.cfm?dirEntryId=311211.
Wang, J., et al., 2011. Effects of xenoestrogens on the expression of vitellogenin (vtg) and cytochrome P450 aromatase (cyp19a and b) genes in zebrafish (Danio rerio) larvae. J. Environ. Sci. Health - Part A Toxic/Hazard. Subst. Environ. Eng. 46 (9), 960–967. https://doi.org/10.1080/10934529.2011.586253.
Wang, Y., Huang, H., Wu, Q., 2014. Characterization of the zebrafish ugt repertoire reveals a new class of drug-metabolizing UDP glucuronosyltransferases. Mol. Pharmacol. 86 (1), 62–75. https://doi.org/10.1124/mol.113.091462.

Warner, R.M., et al., 2022. Toxicokinetic modeling of per- and polyfluoroalkyl substance concentrations within developing zebrafish (Danio rerio) populations. Environ. Sci. Technol. 56 (18), 13189–13199. https://doi.org/10.1021/acs.est.2c02942.

WebPlotDigitizer - Extract data from plots, images, and maps (no date). . Available at: https://automeris.io/WebPlotDigitizer/(Accessed: 9 November 2020).

WHO/UNEP, 2012. State of the science of endocrine disrupting chemicals. https://www.who.int/publications-detail-redirect/9789241505031. (Accessed 2 November 2022).

Wiegand, C., et al., 2000. Uptake, toxicity, and effects on detoxication enzymes of atrazine and trifluoroacetate in embryos of zebrafish. Ecotoxicol. Environ. Saf. 45 (2), 122–131. https://doi.org/10.1006/eesa.1999.1845.

Wu, M., et al., 2017. Bioconcentration pattern and induced apoptosis of bisphenol A in zebrafish embryos at environmentally relevant concentrations. Environ. Sci. Pollut. Control Ser. 24 (7), 6611–6621. https://doi.org/10.1007/s11356-016-8351-0.

Yang, J., et al., 2019. Graphene Oxide Mitigates Endocrine Disruption Effects of Bisphenol A on Zebrafish at an Early Development Stage, vol. 697. Science of The Total Environment, 134158. https://doi.org/10.1016/j.scitotenv.2019.134158.

Zhang, D., Zhou, E., Yang, Z., 2017. Waterborne exposure to BPS causes thyroid endocrine disruption in zebrafish larvae. PLoS One 12 (5), e0176927. https://doi.org/10.1371/journal.pone.0176927.